DOE/NASA/51040-33
NASA TM-82727

NASA-TM-82727 19820004120

Jet Impingement Heat Transfer Enhancement for the GPU-3 Stirling Engine

Douglas C. Johnson, Craig W. Congdon,
Lester L. Begg, and Edward J. Britt
Rasor Associates, Inc.

and

Lanny G. Thieme
National Aeronautics and Space Administration
Lewis Research Center

October 1981

Prepared for
U.S. DEPARTMENT OF ENERGY
Conservation and Renewable Energy
Office of Vehicle and Engine R&D

DOE/NASA/51040-33
NASA TM-82727

Jet Impingement Heat Transfer Enhancement for the GPU-3 Stirling Engine

Douglas C. Johnson, Craig W. Congdon,
Lester L. Begg, and Edward J. Britt
Rasor Associates, Inc.
Sunnyvale, California 94086

and

Lanny G. Thieme
National Aeronautics and Space Administration
Lewis Research Center
Cleveland, Ohio 44135

October 1981

Work performed for
U.S. DEPARTMENT OF ENERGY
Conservation and Renewable Energy
Office of Vehicle and Engine R&D
Washington, D.C. 20545
Under Interagency Agreement DE-AI01-77CS51040

N82-11993#

SUMMARY

In support of the Department of Energy's Stirling Engine Highway Vehicle Systems Program, this investigation demonstrated the benefits resulting from enhanced combustion-gas-side heat transfer using jet impingement in the GPU-3 Stirling engine. A computer model of the combustion-gas-side heat transfer was developed to predict the effects of a jet impingement system and the possible range of improvements available. A low temperature (315°C (600°F)) pretest was run on the GPU-3 heater head to verify the jet impingement model and to improve the correlation coefficients in the model. Utilizing the pretest data in an updated model, a high temperature silicon carbide jet impingement heat transfer system was designed and fabricated.

The system model predicted that at the theoretical maximum limit, jet impingement enhanced heat transfer can: 1) reduce the flame temperature by 275°C (500°F), 2) reduce the exhaust temperature by 110°C (200°F), and 3) increase the overall heat into the working fluid by 10%, all for an increase in required pumping power of less than 0.5% of the engine power output. Initial tests on the GPU-3 Stirling engine at NASA-Lewis demonstrated that the jet impingement system increased the engine output power and efficiency by 5% - 8% with no measurable increase in pumping power. The overall heat transfer coefficient was increased by 65% for the maximum power point of the tests.

Preliminary cost estimates indicate that addition of jet impingement to the system will cost less than $50/unit on a production basis. On the basis of improved engine performance for minimal additional cost, jet impingement is an attractive addition to the design of advanced Stirling engines.

INTRODUCTION

This work was performed in support of the U.S. Department of Energy's (DOE) Stirling Engine Highway Vehicle Systems Program. The NASA Lewis Research Center, through Interagency Agreement DEAI01-77CS51040 with DOE, is responsible for management of the project under the programmatic direction of the DOE Office of Vehicle and Engine R&D, Conservation and Renewable Energy.

The Stirling Engine Highway Vehicle Systems Program is directed toward the development of the Stirling engine as a possible alternative to the conventional spark-ignition engine. A part of this program is development of component technology that will improve engine efficiency and performance for advanced Stirling engine systems.

Of the many factors influencing the performance of a Stirling engine, that of transferring the combustion gas heat into the working fluid is crucial. In a conventional Stirling engine, the heat transfer coefficient on the combustion-gas-side of the heat exchanger, coupled with the combustion gas temperature and heater-tube metal temperature, determines the amount of heater tube surface area required. An increase in the heat transfer coefficient allows either the flame temperature or the heater tube surface area and engine nonswept volume to be reduced. Although the Stirling engine has relatively low exhaust emissions, further reduction is possible if the combustion temperature is reduced.

An illustration of the jet impingement concept is presented in Figure 1. Combustion gas inside a silicon carbide jet shell is forced through holes in the shell, impinging on the heater tubes. The purpose of the directed jets is to break up the boundary layer on the surface of the tubes and thereby reduce the resistance to heat transfer. The hot jet shell also provides some additional radiant heat transfer to the heater tubes.

Rasor Associates has applied jet impingement heat transfer to other high temperature combustion systems (ref. 1, 2). Figure 2 shows a combustion-heated silicon carbide jet impingement shell used in thermionic converter testing and Figure 3 illustrates the effect of tailoring the heat flux. Based on this experience, a jet impingement heat transfer system was designed for the GPU-3 Stirling engine on test at NASA-Lewis. The purpose of this effort was to verify the possible application of a jet impingement system to a Stirling engine and to quantitatively demonstrate the system performance.

The primary goal of this investigation was to enhance the combustion-gas-side heat transfer using the existing heater head, thereby improving the unmodified engine performance. Once the benefits of jet impingement were verified, a follow-on project would design a heater head to take full advantage of a jet impingement system. Because a smaller amount of heater tube area would be required, the redesign would reduce the non-swept volume in the engine. This would yield a greater performance improvement than retrofitting the existing engine system.

DESIGN OF THE JET IMPINGEMENT SYSTEM

A. Heat Transfer Design

In order to predict the gas temperatures and heat transfer rates necessary for the design of the jet impingement system, a computer model (for a HP9825 desk-top computer) of the combustion gas flow path was developed. In comparing the model to available data, it was noted that the calculated temperatures are a strong function of the preheater effectiveness. Figures 4 and 5 show the heat balance calculated for the NASA reference run, at two different values of preheater effectiveness. Note the decrease in the flame temperature and corresponding increase in heat transfer coefficient for a decrease in preheater effectiveness. The performance of the preheater degrades during operation due to fouling, and there is a corresponding decrease in the effectiveness. Therefore, in order to make a comparison of heat transfer coefficients, tests must be made both with and without jet impingement for a constant preheater condition.

As illustrated in Figure 1, the impinging jets break up the boundary layer on the surface of the heater tubes and cause relatively high local heat transfer coefficients (ref. 3, 4). For an average jet impingement heat transfer coefficient of 880 $W/m^2 {}^\circ C$ and an average tube temperature of 773°C (1423°F), a finite element analysis of the local temperatures under the jet was performed. The results are shown in Figure 6. Although the local heat transfer coefficient varies widely under the jet, the temperature variation in this region is less than 55°C (100°F).

B. Hardware Design

To contain the hot combustion gases and form the jets which impinge on the heater tubes, a silicon carbide jet shell was designed. Figure 7 shows the GPU-3 Stirling engine heater head/jet shell assembly. As shown in Figure 8, the jets impinge directly on the heater tubes. To compensate for differences in thermal expansion between the heater head and the silicon carbide jet shell, the shell expands to maintain proper alignment at all times. The alignment detail is shown in Figure 9, indicating both the assembled and operating conditions.

Silicon carbide was selected for the jet shell material due to its ability to sustain continued high operating temperatures and its excellent thermal shock resistance. The holes in the jet shell were drilled with a laser because silicon carbide cannot be machined economically by conventional techniques. A photo taken during the laser drilling operation is shown in Figure 10.

PRETEST

Predictions of jet impingement heat transfer coefficients are based on correlations made in terms of Reynolds number, Nusselt number, Prandtl number, and geometric variables such as jet spacing and hole diameter (refs. 3-6). A pretest was performed on the GPU-3 heater head to verify and improve the correlation coefficients used to predict jet impingement heat transfer.

A stainless steel mockup jet shell (Figure 11) with geometric variables within the range expected in the final design was fabricated. In order to simulate the heater head operation without risk of damage to the heater head, air heated to 315°C (600°F) from an electrically heated pipe was blown past the heater tubes as shown schematically in Figure 12. Since the heater head consists of four identical sections, only one quadrant (1/4 of heater head) was used for the flow tests. The effect of jet impingement as measured in this pretest is shown in Figure 13, clearly showing the improved heat transfer with jet impingement.

Based on the pretest results, a new prediction of jet impingement heat transfer in the heater head was made for the NASA baseline case presented in Figure 14 for a preheater effectiveness of 80%. The engine conditions for this case were as follows: mean compression-space pressure, 6.9MPa (1000 psi); engine speed, 3000 rpm; air-fuel ratio, 26 to 1; and working fluid, hydrogen. The potential for enhanced heat transfer at this operating point is shown in Figure 15 assuming the same air and fuel flow rates and heater tube temperature. For a small penalty in pumping power (less than 0.5% of engine output), the computer model indicates that at the theoretical maximum limit, jet impingement enhanced heat transfer should: 1) reduce the flame temperature by 275°C (500°F), 2) reduce the exhaust temperature by 110°C (200°F), and 3) increase the overall heat into the working fluid by 10%. The theoretical maximum limit is defined as the point where the combustion gas temperature leaving the heater tubes equals the temperature of the tubes.

Based on the pretest results, the final design of the jet impingement system was completed. Figure 16 shows the components of the jet impingement system (upper retaining ring is not shown), and Figure 17 shows the jet shell installed in the heater head. The final dimensions for the shell are given in Figures 8 and 9. There are 14 jet impingement holes per heater tube; the overall weight of the shell is 245 grams (0.54 lb).

DEMONSTRATION

To demonstrate the effects of the jet impingement heat transfer system, tests were performed at NASA-Lewis on the GPU-3 Stirling engine for similar operating points both with and without jet impingement. The operating points were 1500 rpm and 2500 rpm at 4.1 MPa (600 psi) mean compression-space pressure for helium working fluid, and 2000 rpm and 3000 rpm at 6.9 MPa (1000 psi) helium pressure. All points were controlled to give 677°C (1250°F) working fluid temperature in the heater and the cooling-water inlet temperature was 21°C (70°F). The heater working fluid temperature was controlled to the maximum reading of thermocouple probes installed inside three of the heater-tubes and spaced circumferentially around the heater head. Data were obtained on the increase in pump power required and engine performance.

The GPU-3 engine tests with the jet impingement system indicated a substantial improvement in overall performance. Representative heat balance computer runs based on the experimental data are shown in Figures 18-19. Inputs for the heat balance are the air and fuel flow rates, the inlet air temperature, nozzle and preheater losses, preheater effectiveness, heat into the engine and the heater-tube metal temperature. A preheater effectiveness of 71% was chosen to give a reasonable match between the calculated and measured temperatures at positions 2, 4, and 5 shown in Figures 18-19. Based on the calculated temperatures at positions 3 and 4, the average measured heater-tube metal temperature and the heat into the engine, the effective heat transfer coefficient was determined. Table 1 summarizes the test results. The run numbers with a "JS" or "J" indicate the tests with the jet impingement shell.

The engine power is increased by 5.9 to 7.7 percent for the runs with jet impingement. The engine pressure, speed, cooling-water inlet temperature, and maximum heater-tube gas temperature were held constant for a given point with and without jet impingement. The increased power output and efficiency therefore were due to the jet shell smoothing the temperature profiles by providing a more uniform heat flux to the heater tubes and thereby raising the average gas temperature. Figures 20 and 21 indicate that both the circumferential temperature profiles around the heater head and the tube vertical temperature profiles were more uniform. The increase in engine efficiency was about the same as the increase in engine output.

Figure 22 shows the increase in overall heat transfer coefficient with jet impingement for the demonstration tests. Both the demonstration test and the pretest (Figure 13) indicate a 65 - 70% increase in the effective heat transfer coefficient. The decrease in exhaust temperature and flame temperature for the jet impingement runs shown in Table 1 are due to this increase in the effective heat transfer coefficient. The absolute values determined from the test are significant only for comparison of the similar cases due to uncertainties in the measured system temperatures. At the maximum power point tested, the relative increase in the heat transfer coefficient was 65 percent and the increase in engine power was 7.4 percent.

Since the overall pumping power in the engine combustion system increases with jet impingement, cold flow tests of the required air pressure, both with and without the jet shell, were performed. Inspection of the data presented in Figure 23 shows that the increase in pressure for the jet impingement system was not discernible. Also, the data taken during the demonstration tests showed the increase in pump power to be insignificant.

CONCLUSIONS

Jet impingement heat transfer has been successfully demonstrated as a technique for enhancing the combustion-gas-side heat transfer in the GPU-3 Stirling engine. The combustion-gas-side heat transfer coefficient was increased by about 65%, along with an increase of the engine power and efficiency by 5 to 8% due to jet impingement. Both the circumferential temperatures around the heater head and the vertical tube temperatures were made more uniform with the jet impingement system. The additional pumping power required with the jet impingement system was insignificant over that required for the baseline case. Preliminary cost estimates indicate that a Stirling engine jet impingement system will cost less than $50 per unit on a mass production basis.

On the basis of improved engine performance for minimal additional cost, the jet impingement system is an attractive addition to the design of advanced Stirling engines. Further work should be undertaken to design a heater head to take full advantage of the jet impingement system.

REFERENCES

1. Begg, L. L. and Fitzpatrick, G. O., "ZEPO - The World's Largest Thermionic Converter," Intersociety Energy Conversion Engineering Conference, 14th, Boston, Mass., Aug. 5-10, 1979, proceedings, Vol. 2, American Chemical Society, Washington, D.C., 1979, pp. 1868-1874.

2. Fitzpatrick, G. O. and Begg, L. L., "High Thermionic Converter Test Facility and Initial Converter Test Results," Rasor Associates, Sunnyvale, Calif., "Topical Report NSR 2-10, Sept. 1978.

3. Gardon, R. and Cobonpue, J., "Heat Transfer Between a Flat Plate and Jets of Air," International Developements of Heat Transfer, Proceedings of the 1961-1962 Heat Transfer Conference, American Society of Mechanical Engineers, New York, 1963, pp. 454-460.

4. Martin, H., "Heat and Mass Transfer Between Impinging Gas Jets and Solid Surfaces," Advances in Heat Transfer, Vol. 13, Academic Press, New York, 1977, pp. 1-60.

5. Kercher, D. M. and Tabakoff, W., "Heat Transfer by a Square Array of Round Air Jets Impinging Perpendicular to a Flat Surface Including the Effect of Spent Air," Journal of Engineering for Power, Vol. 92, No. 1, 1970, pp. 73-82.

6. Hollworth, B. R. and Berry, R. D., "Heat Transfer from Arrays of Impinging Jets with Large Jet-to-Jet Spacing," ASME paper no. 78-GT-117, May 1978.

TABLE 1. GPU-3 TEST RESULTS

PREHEATER EFFECTIVENESS = 71%													
			TEMPERATURE (°C)								% INCREASE DUE TO JET IMPINGEMENT		
RUN NUMBER	HELIUM PRESSURE (MPa)	ENGINE SPEED (RPM)	MEASURED EXHAUST	CALCULATED EXHAUST	CALCULATED FLAME	TUBE	HEAT INTO ENGINE (W)	ENGINE POWER (kW)	ENGINE EFFICIENCY	EFFECTIVE HT. TRANS COEF ($W/m^2 °C$)	POWER	EFFICIENCY	HT. TRANS
HE25-65	4.1	1500	244	234	1765	698	7791	1.871	18.81	218			
HE25-65JS	4.1	1500	239	230	1699	711	7852	2.015	19.86	272	7.7	5.6	24.1
HE25-63	4.1	2500	251	239	1719	706	12301	2.306	14.86	417			
HE25-63JS	4.1	2500	242	230	1722	719	12350	2.488	15.98	603	7.2	7.5	44.5
HE25-104	6.9	2000	264	250	1726	717	15109	3.803	19.88	474			
HE25-104J	6.9	2000	252	239	1704	729	15450	4.028	20.85	808	5.9	4.9	70.3
HE25-102	6.9	3000	291	273	1766	742	21214	4.025	14.82	577			
HE25-102J	6.9	3000	270	254	1712	759	21462	4.324	15.84	954	7.4	6.9	65.3

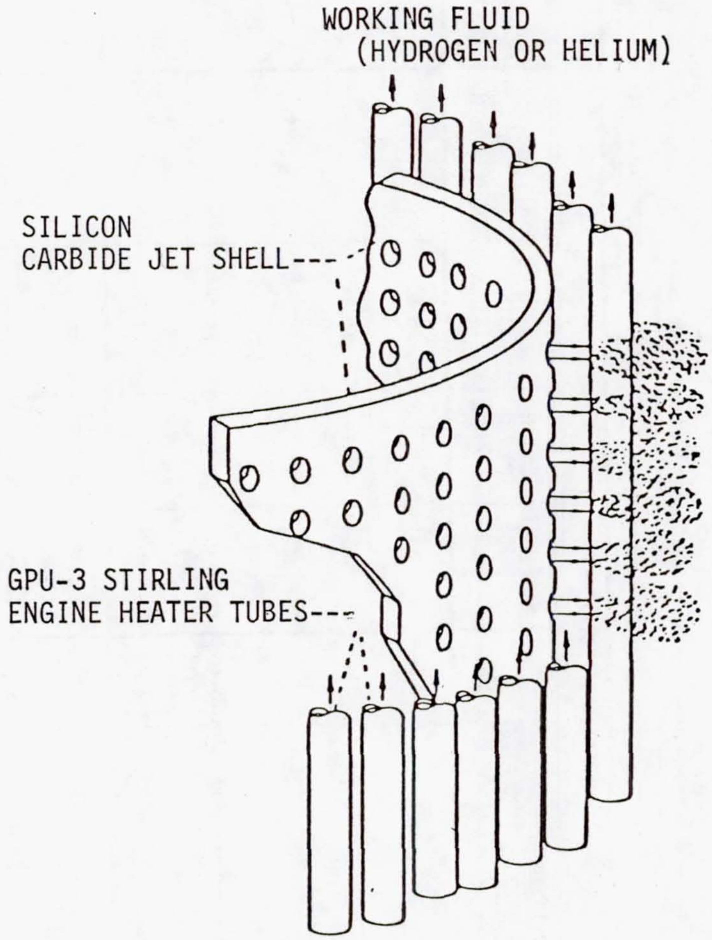

Fig. 1 Schematic of jet impingement concept.

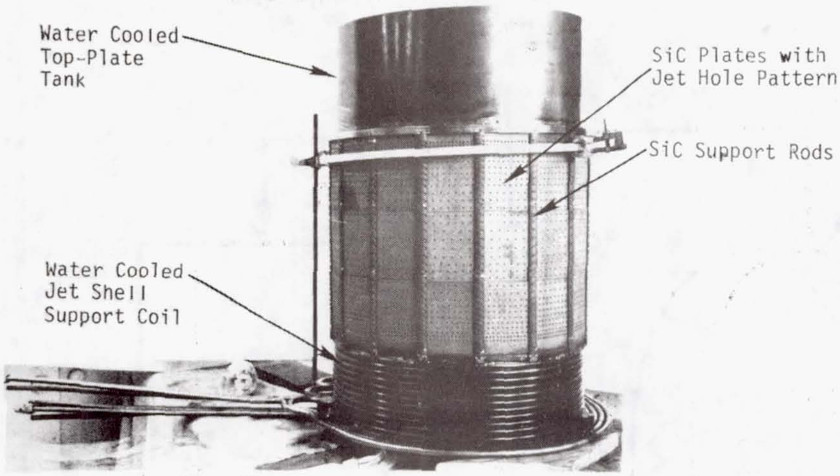

Fig. 2 Combustion-heated SiC jet impingement shell used in thermionic converter testing. This shell delivered 193,370 Btu/hr-ft^2 (61 W/cm^2) at 1652°F (900°C).

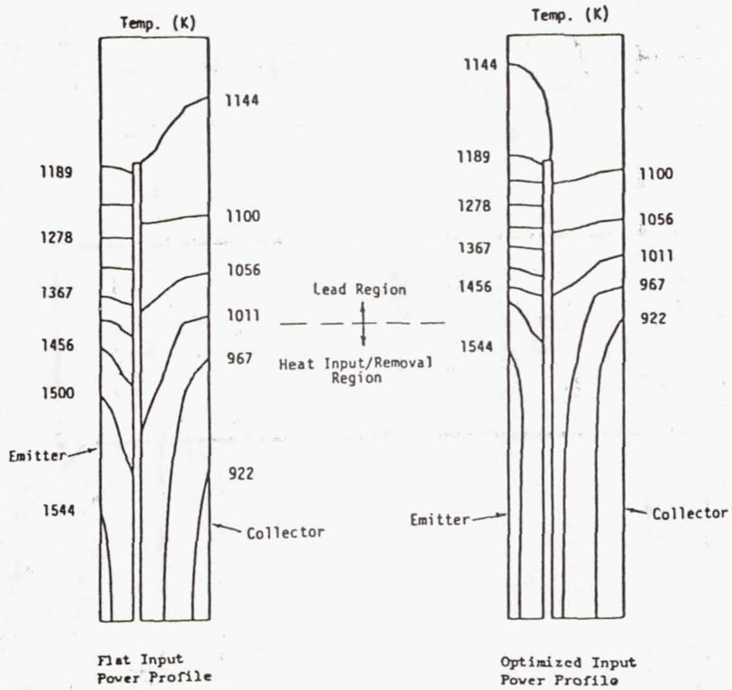

Fig. 3 Effect of tailoring heat flux profile on temperature by using jet impingement.

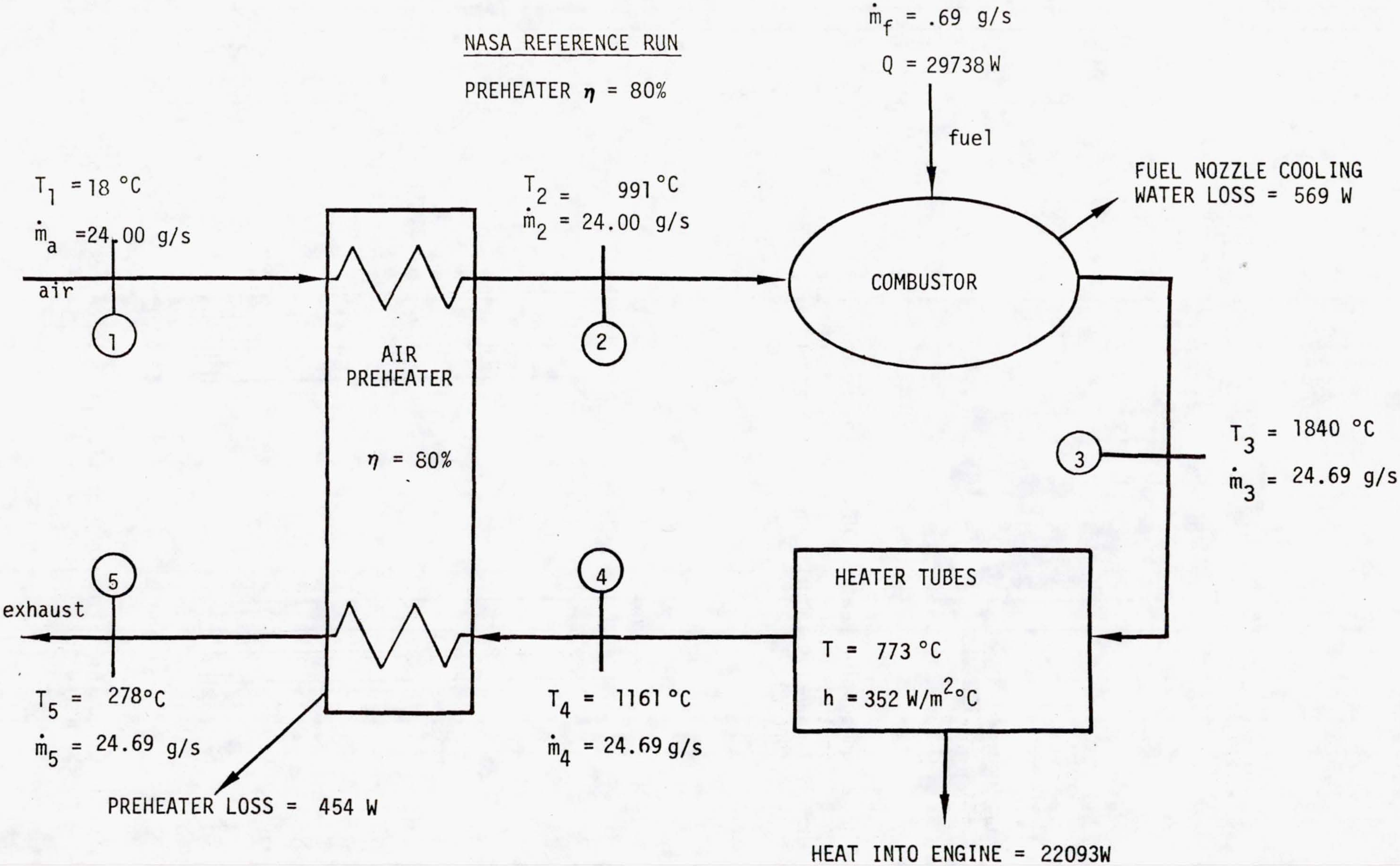

Figure 4. NASA reference heat balance assuming a preheater effectiveness of 80%.

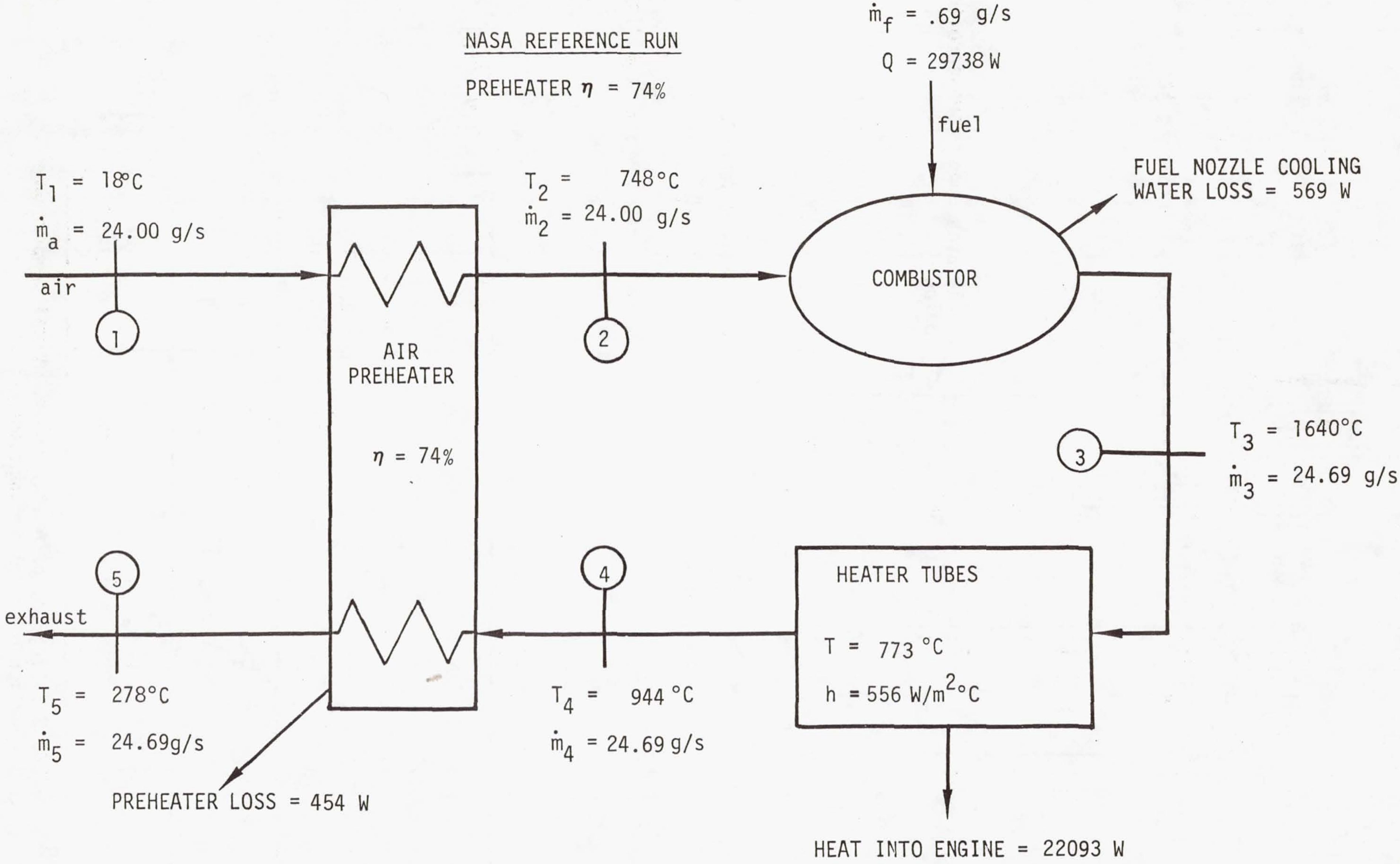

Figure 5. NASA reference heat balance assuming a preheater effectiveness of 74%.

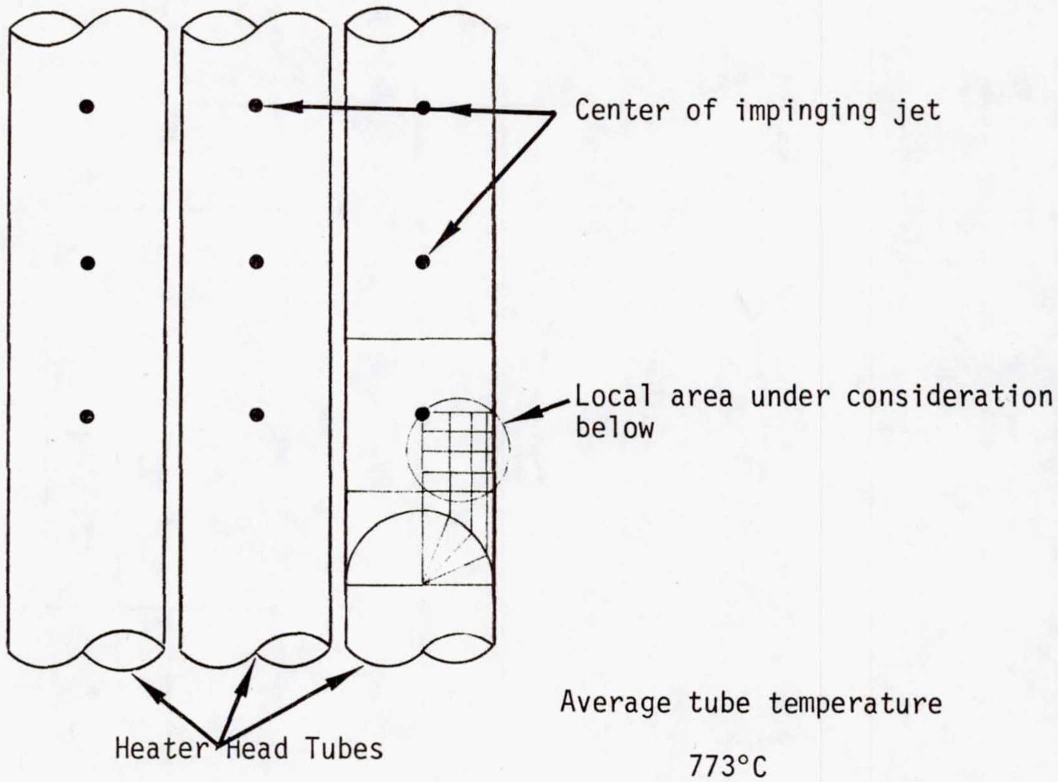

Average tube temperature

773°C

Average heat transfer coefficient

880 W/ m^2°C

Local Temperatures and Convection Coefficients

h = 1192 T = 801	h = 1050 T = 791	h = 624 T = 776	h = 426 T = 767	h [W/ m^2°C] T [°C]
h = 1164 T = 798	h = 999 T = 788	h = 454 T = 772	h = 341 T = 761	
h = 1022 T = 793	h = 903 T = 783	h = 255 T = 766	h = 85 T = 757	
h = 681 T = 787	h = 545 T = 778	h = 170 T = 762	h = 57 T = 753	

Figure 6. GPU-3 Stirling Engine heater tubes. Local temperature distribution with jet impingement.

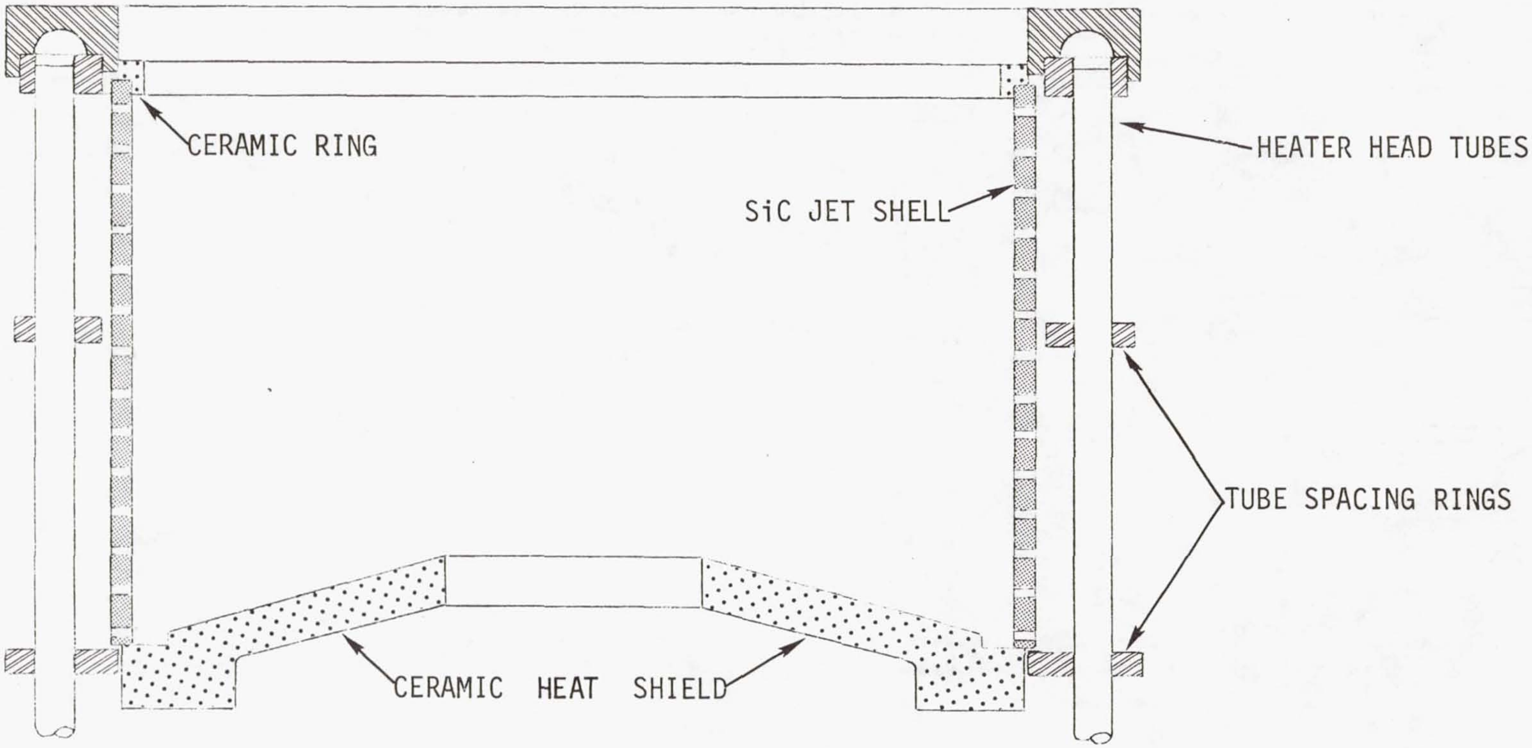

Figure 7. GPU-3 Stirling engine heater head/jet shell assembly.

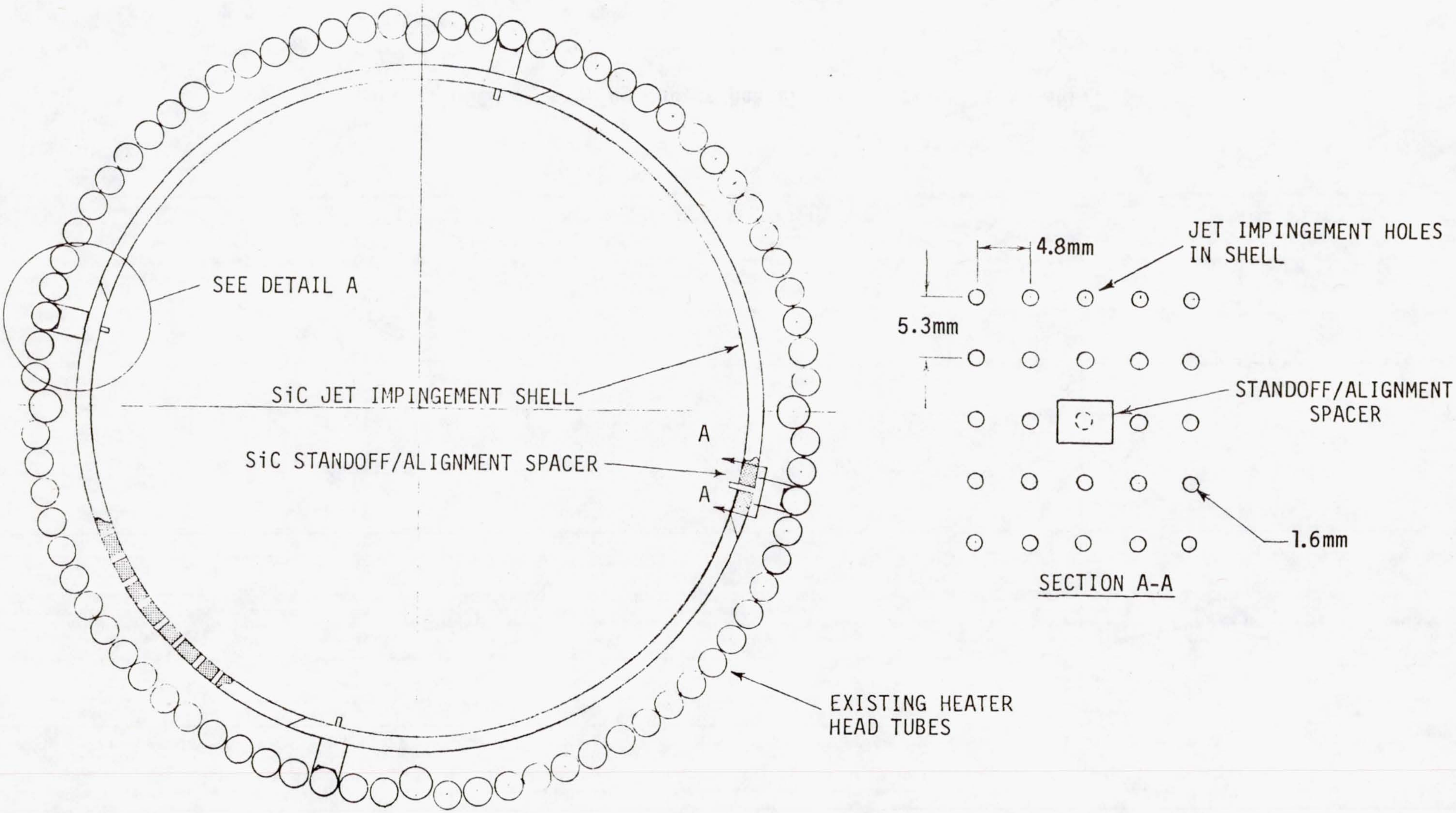

Figure 8. Top view of jet shell assembly.

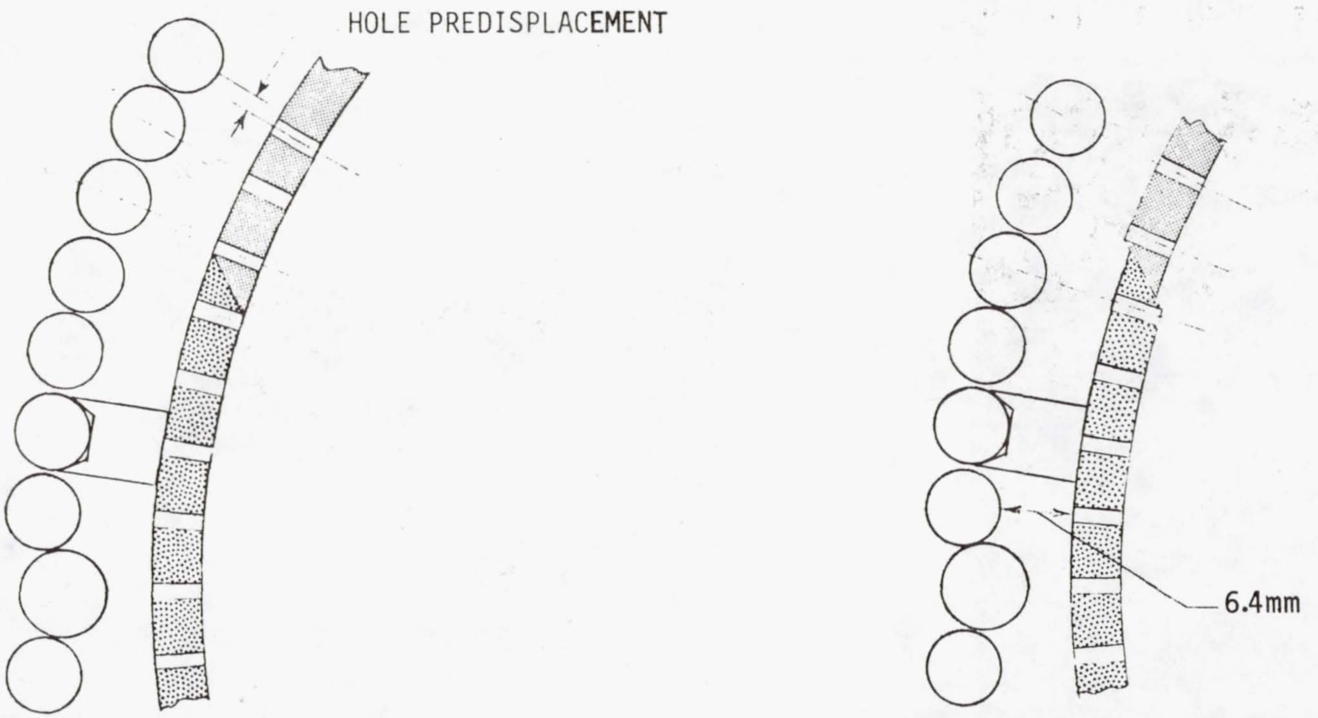

POSISTION OF BEVEL JOINT AND PREDISPLACEMENT
OF HOLES IN "AS ASSEMBLED" CONDITION

POSITION OF BEVEL JOINT AND HOLE ALIGNMENT
DURING OPERATING CONDITIONS

Figure 9. Detail A illustrating hole alignment.

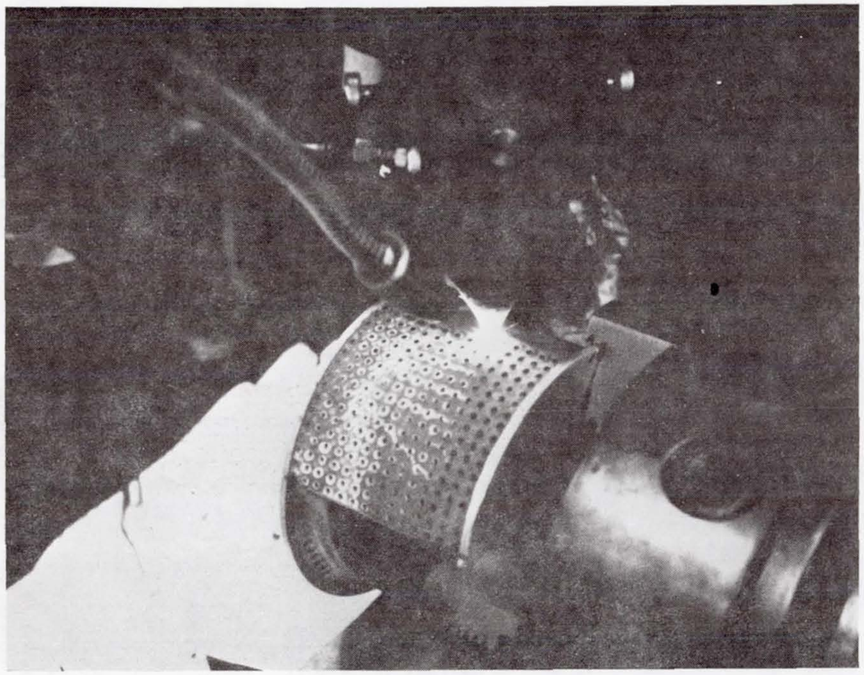

Figure 10. Laser drilling holes in SiC jet shell.

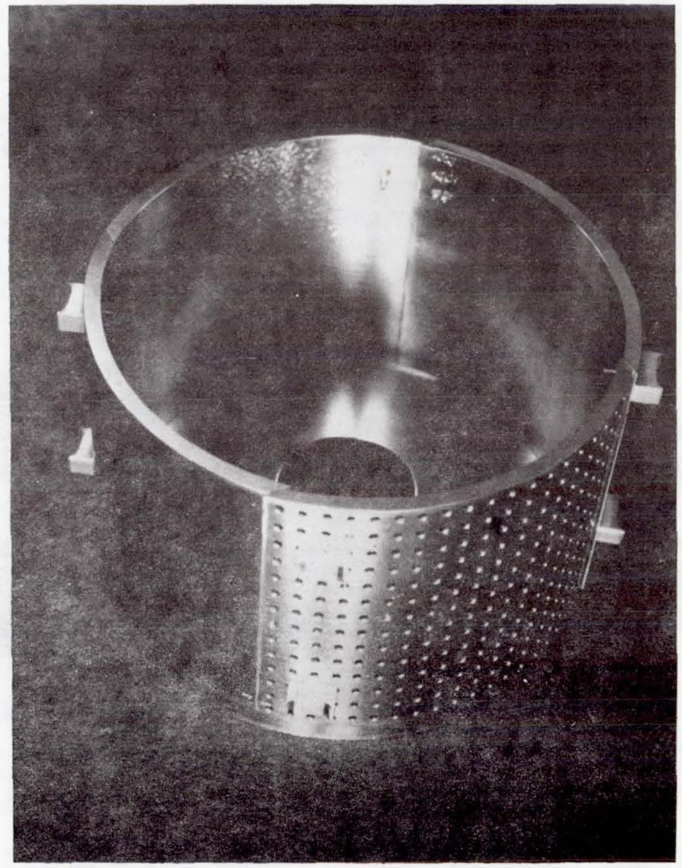

Figure 11. Stainless steel mockup jet shell.

STIRLING ENGINE PRETEST
Test Set-up

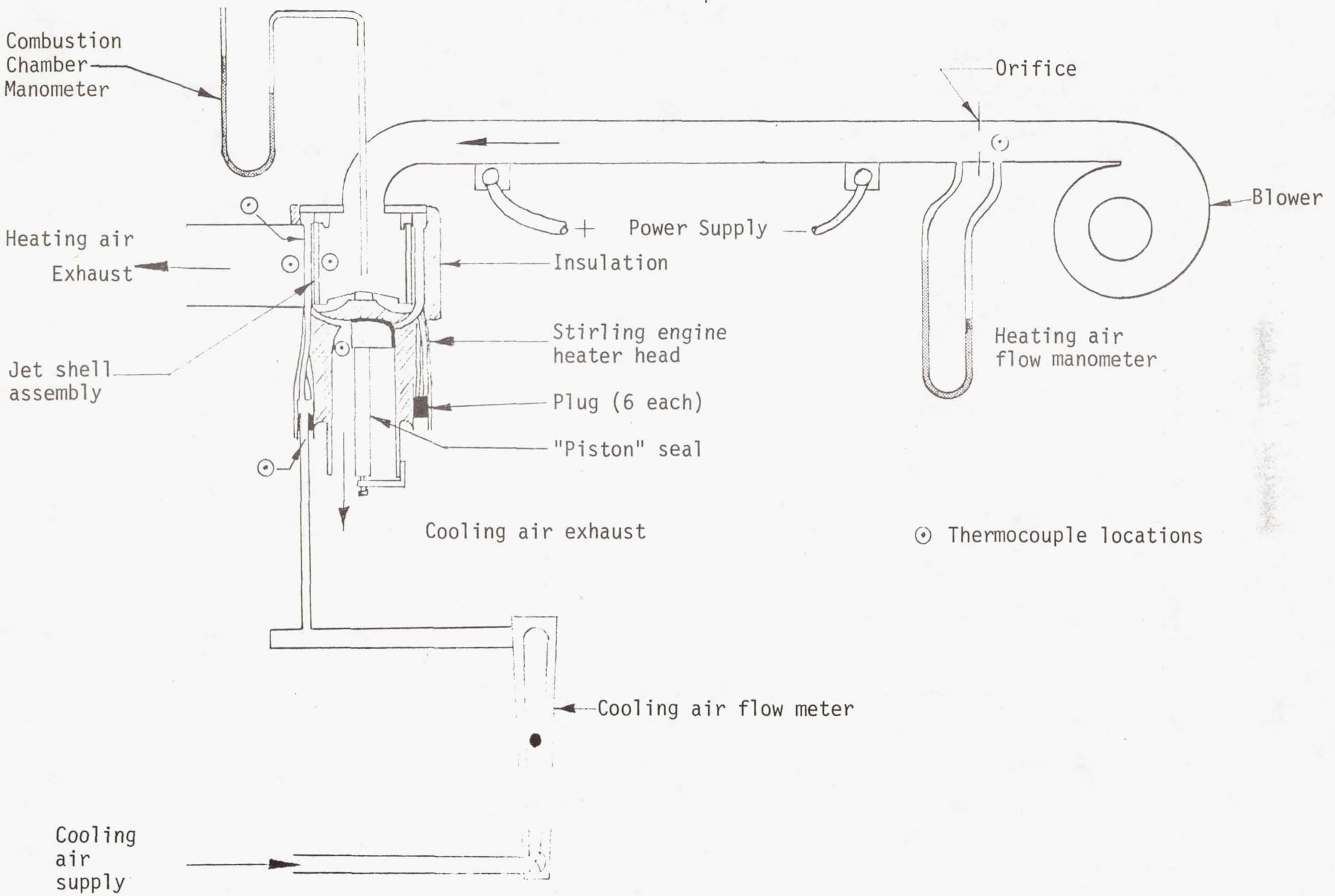

Fig. 12 Stirling engine pretest: Test schematic.

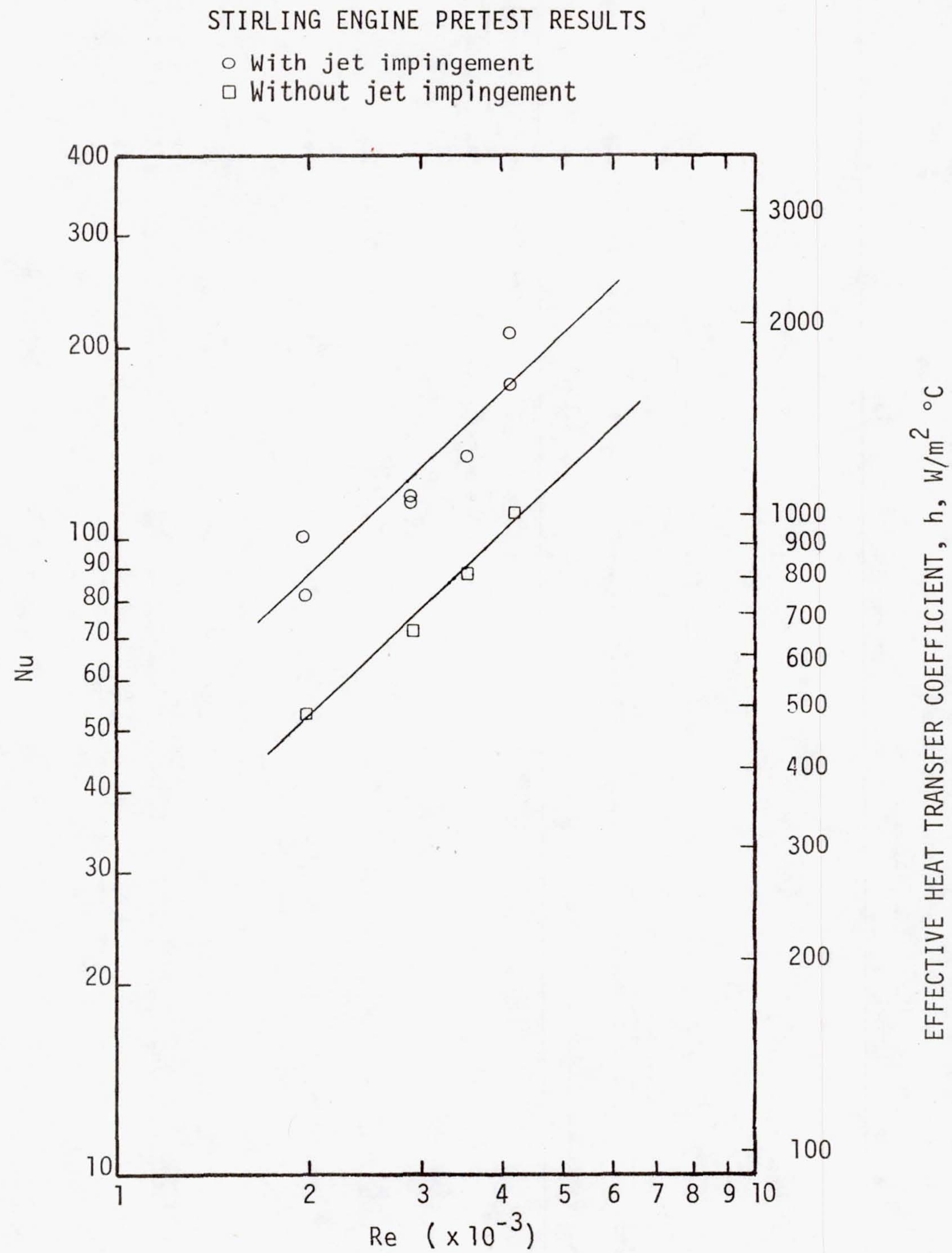

Fig. 13 Heat transfer enhancement due to jet impingement.

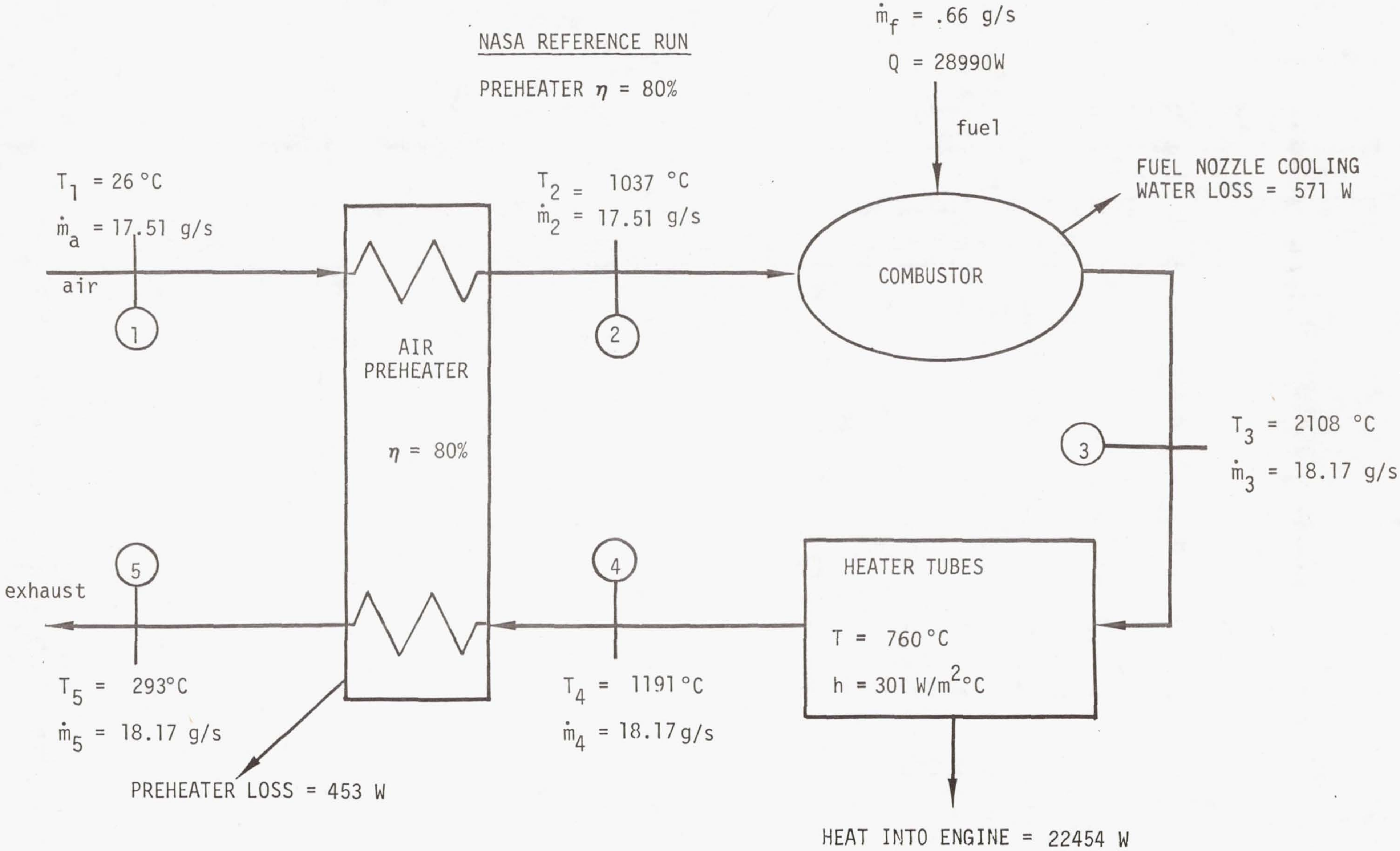

Figure 14. NASA baseline case assuming a preheater effectiveness of 80%.

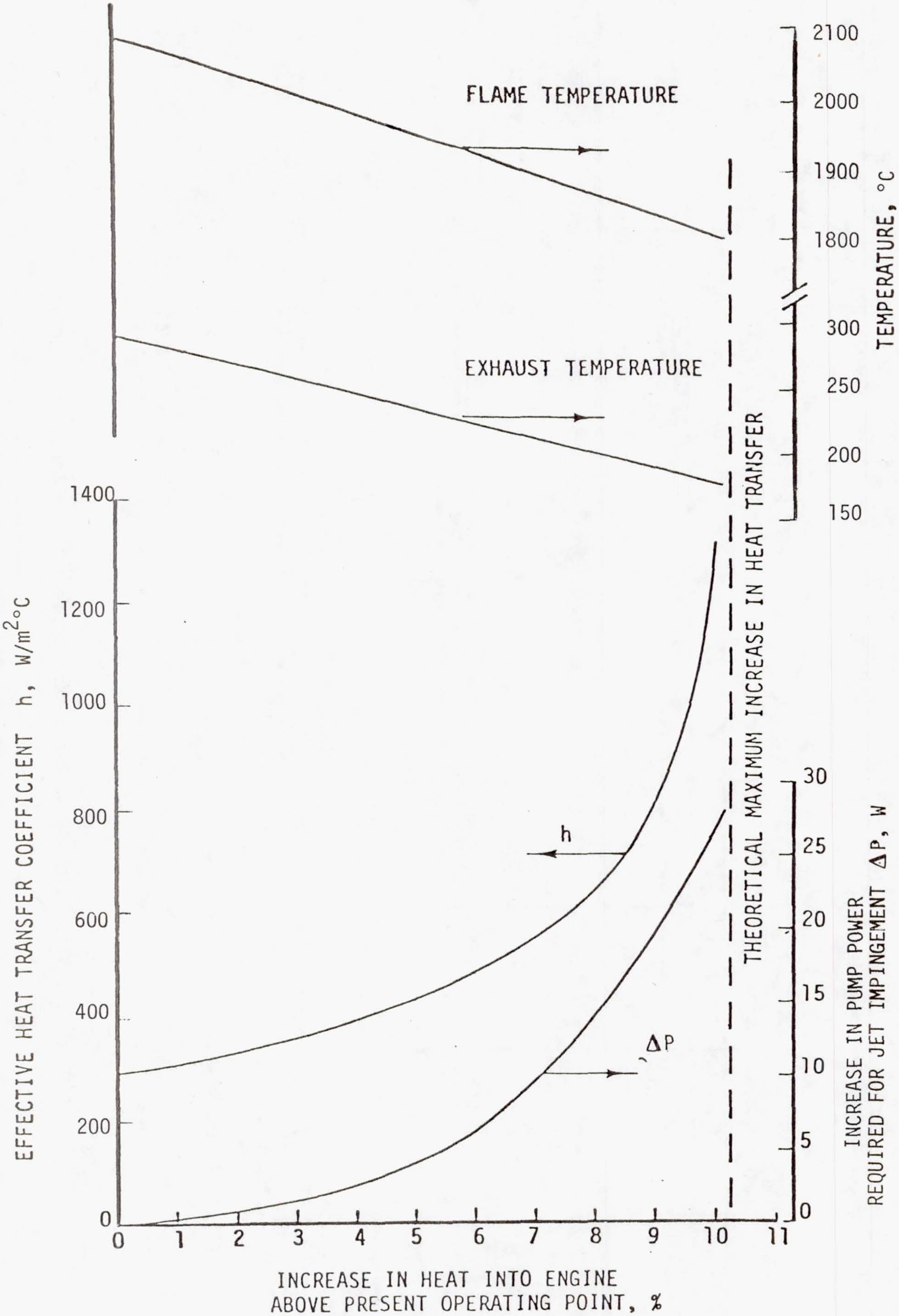

Figure 15. PREDICTED EFFECTS OF JET IMPINGEMENT FOR THE GPU-3 STIRLING ENGINE.

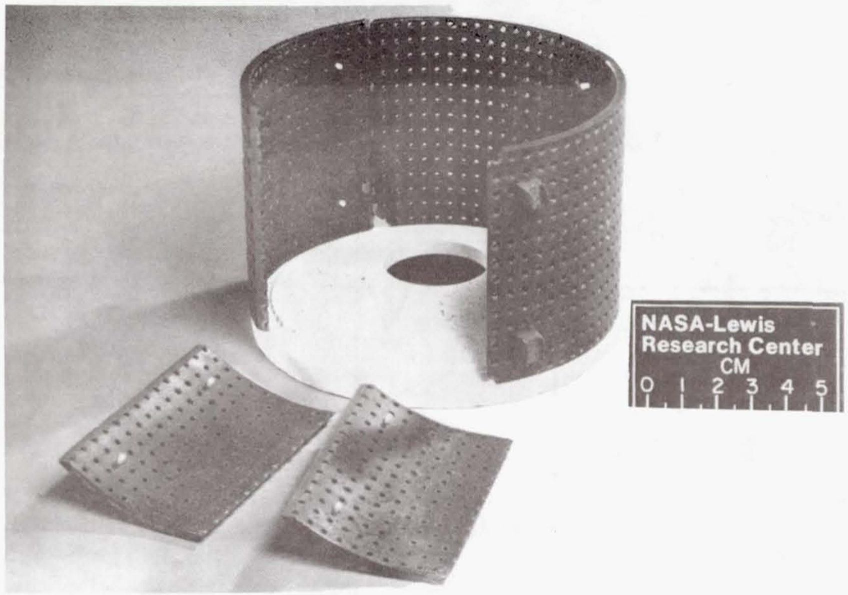

Figure 16. SiC jet shell.

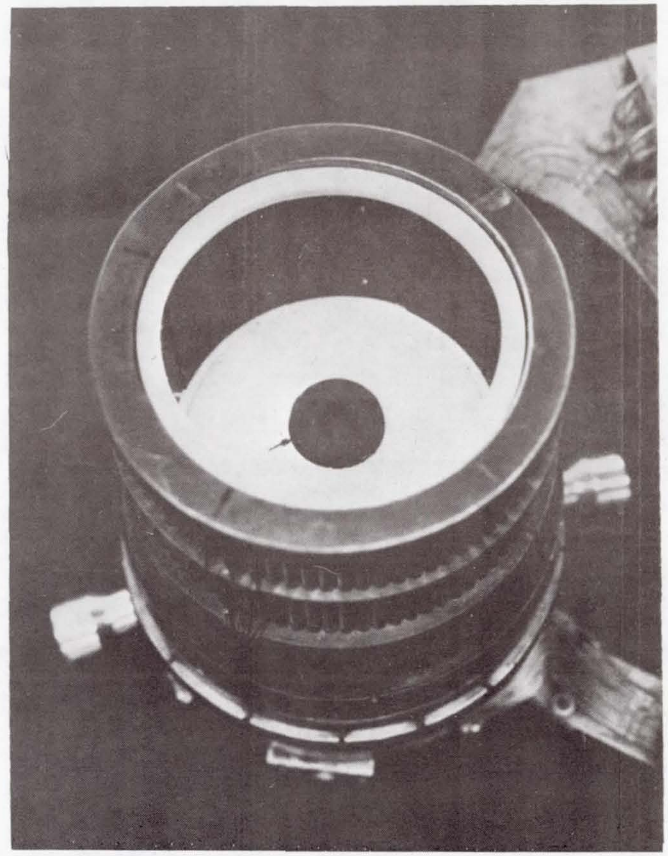

Figure 17. SiC jet shell installed in heater head.

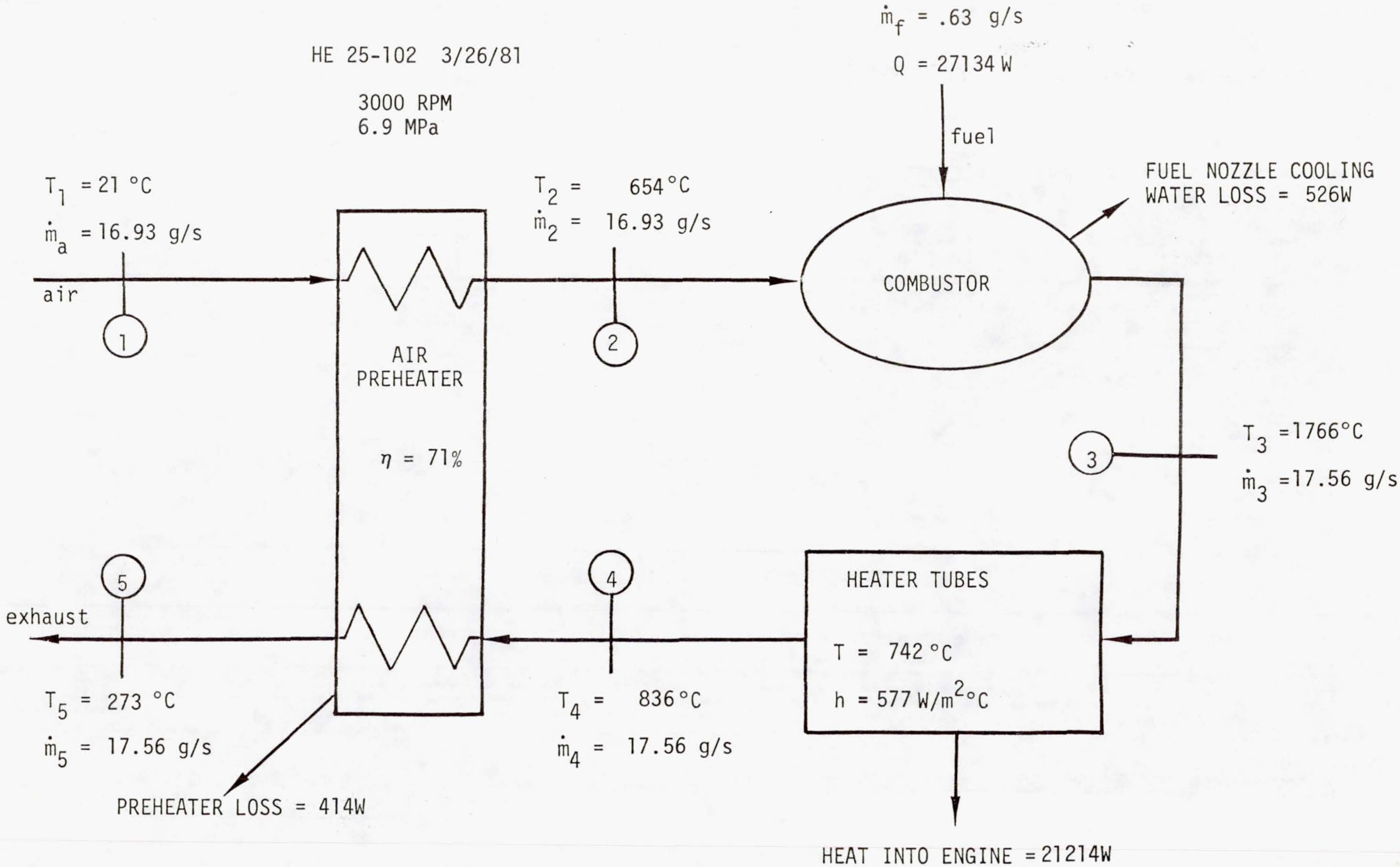

Figure 18. Heat balance based on experimental data. Baseline run without jet impingement.

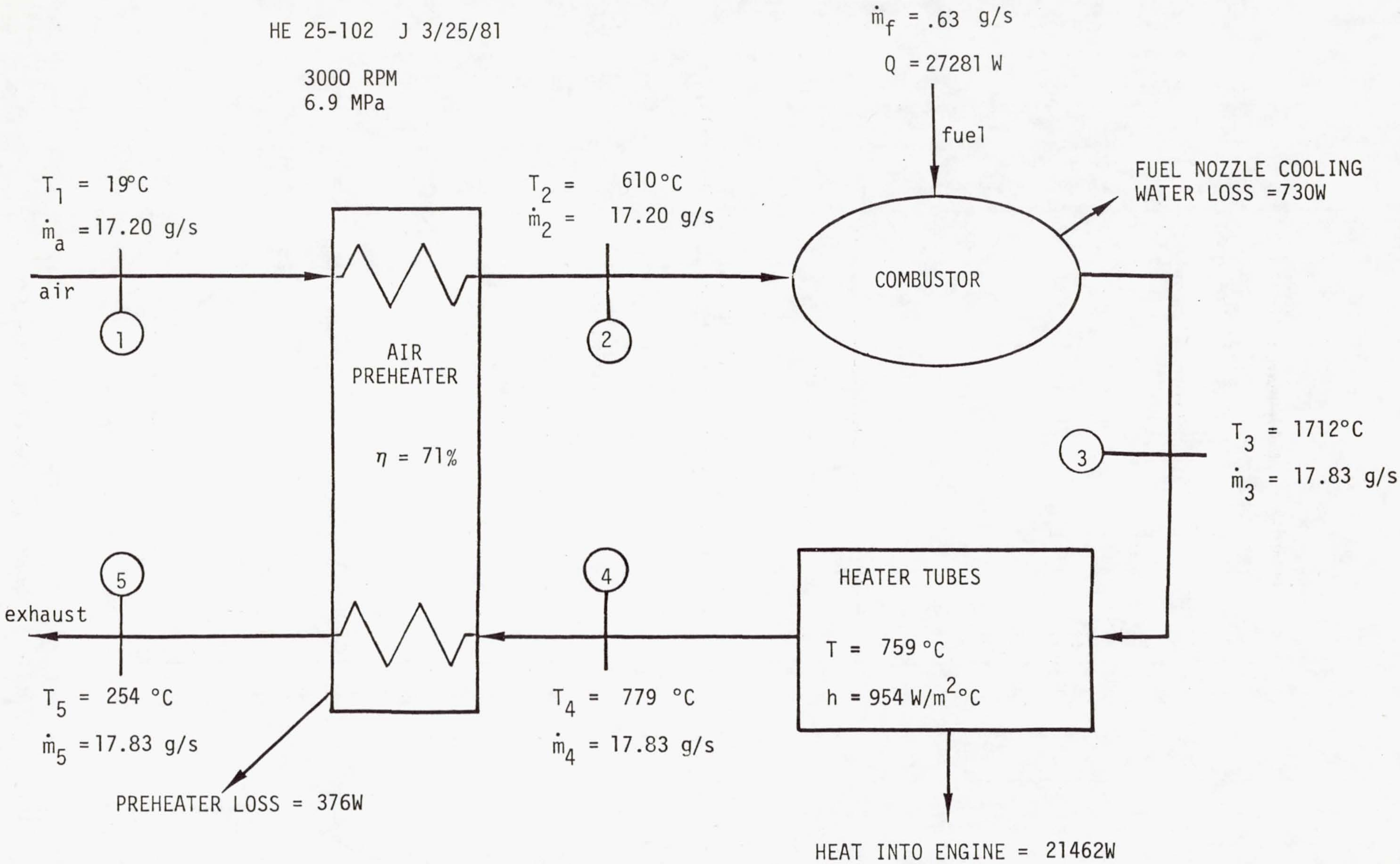

Figure 19. Heat balance based on experimental data. Baseline run with jet impingement.

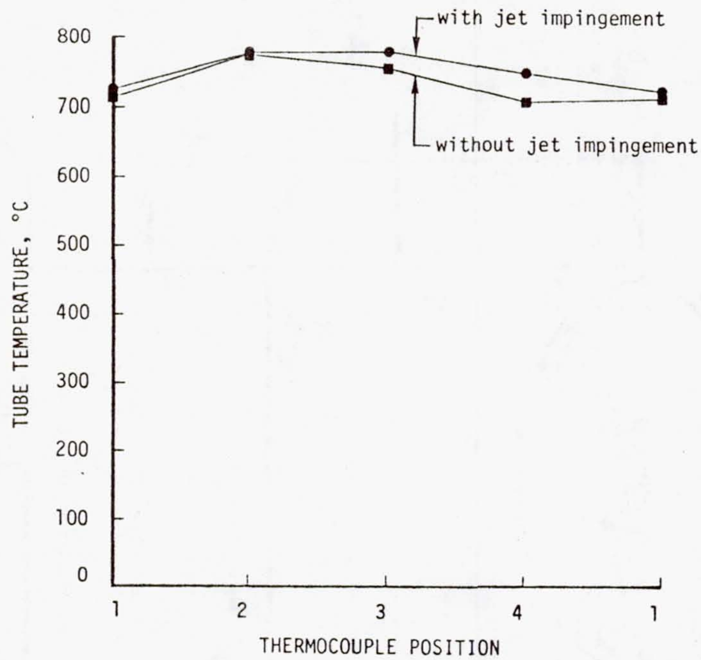

Figure 20. Circumferential heater-tube metal temperatures. Thermocouples are located around the heater head at 90° intervals.

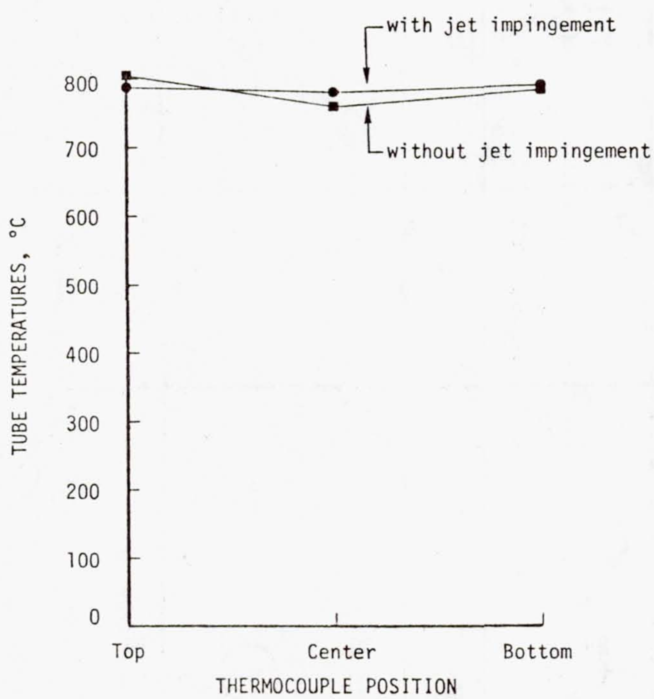

Figure 21. Vertical heater-tube metal temperatures.

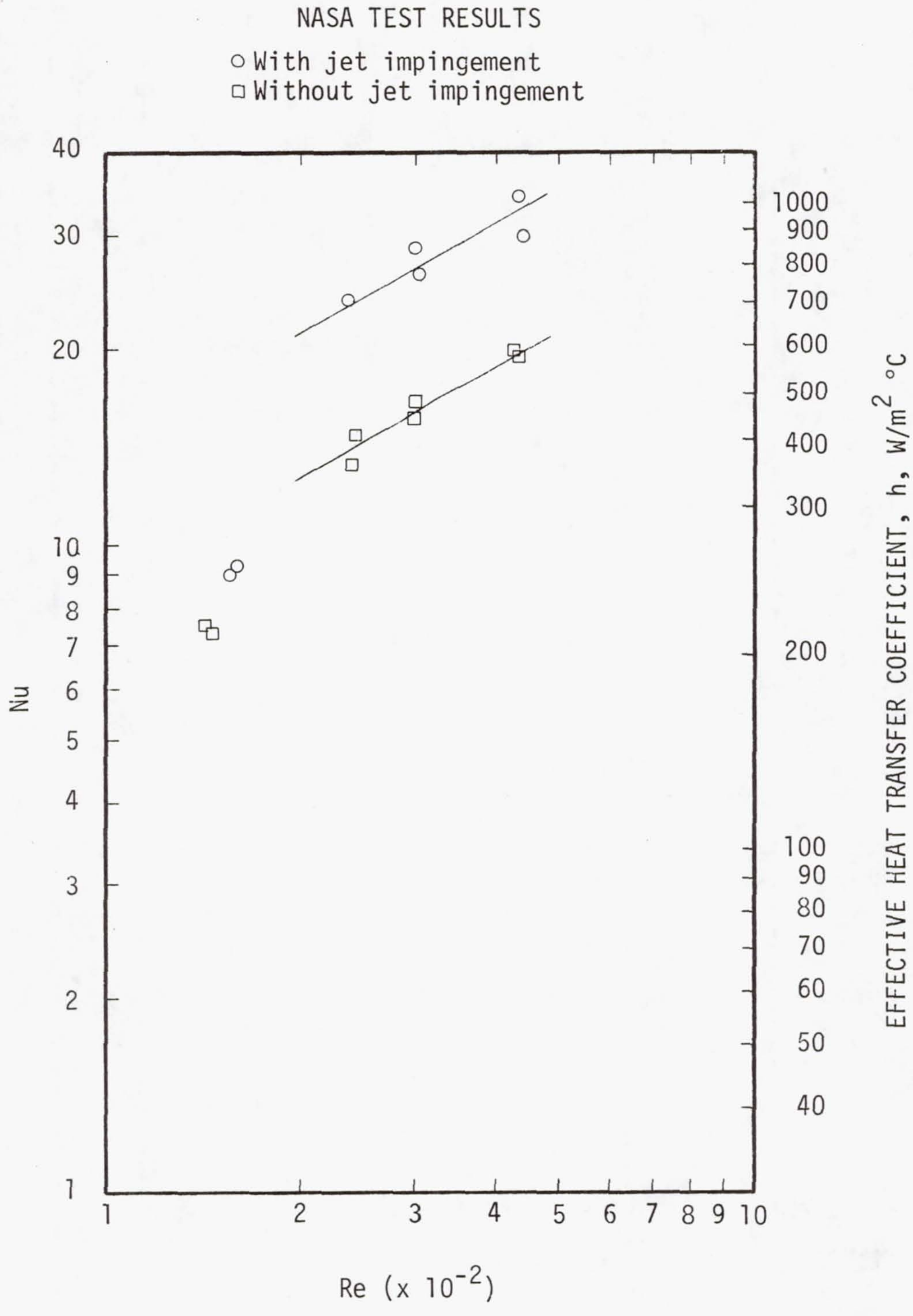

Fig. 22 Heat transfer enhancement due to jet impingement in the GPU 3 Stirling engine.

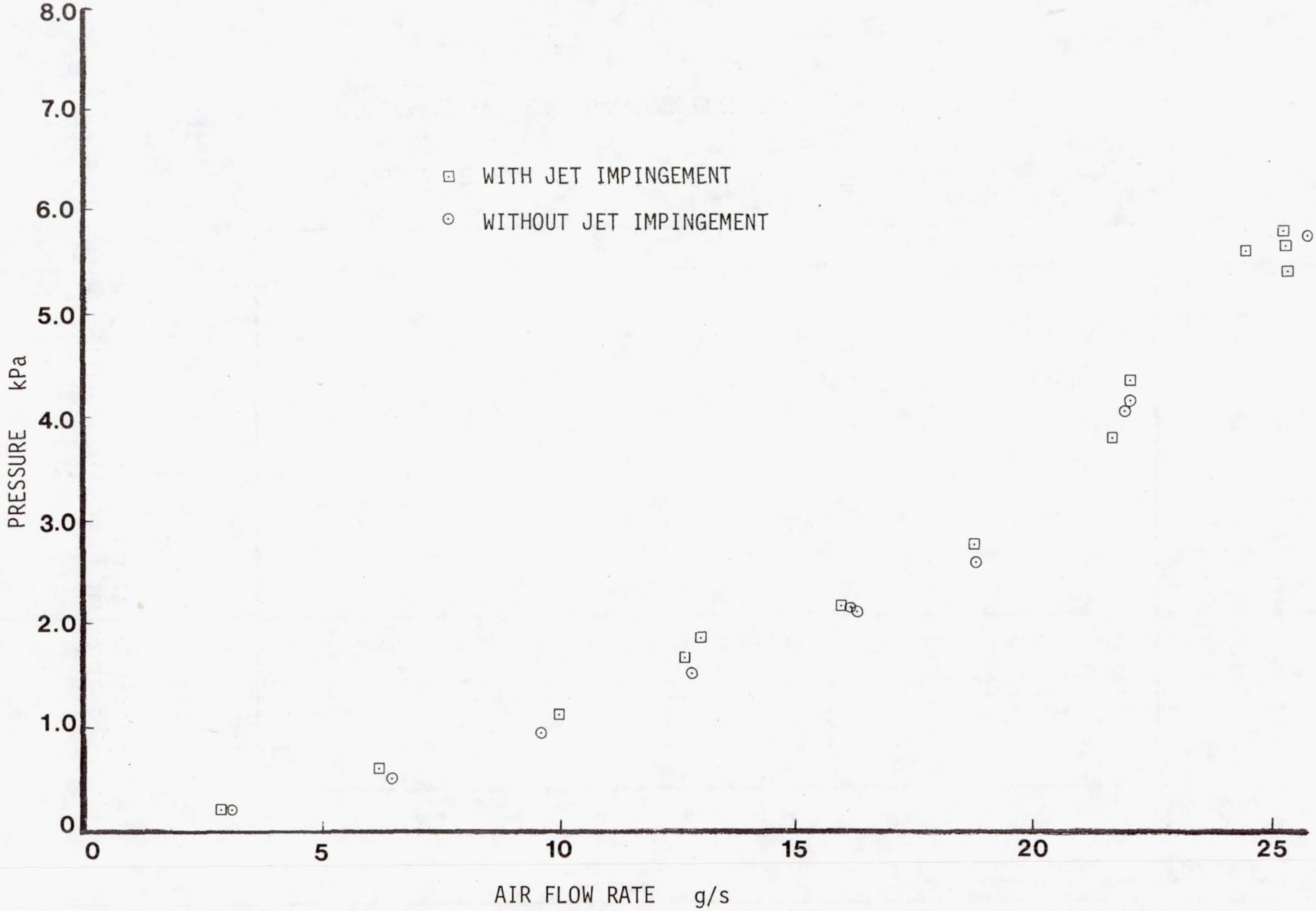

Figure 23. GPU-3 cold flow pressure drop results.

1. Report No.	2. Government Accession No.	3. Recipient's Catalog No.
NASA TM-82727		
4. Title and Subtitle JET IMPINGEMENT HEAT TRANSFER ENHANCEMENT FOR THE GPU-3 STIRLING ENGINE		5. Report Date October 1981
		6. Performing Organization Code 778-35-03
7. Author(s) Douglas C. Johnson, Craig W. Congdon, Lester L. Begg, and Edward J. Britt, Rasor Associates, Inc., and Lanny G. Thieme, Lewis Research Center		8. Performing Organization Report No.
		10. Work Unit No.
9. Performing Organization Name and Address National Aeronautics and Space Administration Lewis Research Center Cleveland, Ohio 44135		11. Contract or Grant No.
		13. Type of Report and Period Covered Technical Memorandum
12. Sponsoring Agency Name and Address U. S. Department of Energy Office of Vehicle and Engine R&D Washington, D.C. 20545		14. Sponsoring Agency ~~Code~~ Report No. DOE/NASA/51040-33
15. Supplementary Notes Final report. Prepared under Interagency Agreement DE-AI01-77CS51040.		

16. Abstract

Of the many factors influencing the performance of a Stirling engine, that of transferring the combustion gas heat into the working fluid is crucial. By utilizing the high heat transfer rates obtainable with a jet impingement heat transfer system, it is possible to reduce the flame temperature required for engine operation thereby resulting in lower exhaust emissions. Also, the required amount of heater tube surface area may be reduced, resulting in a decrease in the engine nonswept volume and related increase in engine efficiency. A jet impingement heat transfer system was designed by Rasor Associates, Inc., and tested in the GPU-3 Stirling engine at the NASA Lewis Research Center. For a small penalty in pumping power (less than 0.5% of engine output) the jet impingement heat transfer system provided a higher combustion-gas-side heat transfer coefficient and a smoothing of heater temperature profiles resulting in lower combustion system temperatures and a 5 to 8% increase in engine power output and efficiency. On the basis of these results, the jet impingement system could be an important contribution to the design of advanced Stirling engines.

17. Key Words (Suggested by Author(s))		18. Distribution Statement	
Jet impingement, Stirling engine, Heat transfer enhancement		Unclassified - unlimited STAR Category 85 DOE Category UC-96	
19. Security Classif. (of this report)	20. Security Classif. (of this page)	21. No. of Pages	22. Price*
Unclassified	Unclassified	27	

* For sale by the National Technical Information Service, Springfield, Virginia 22161